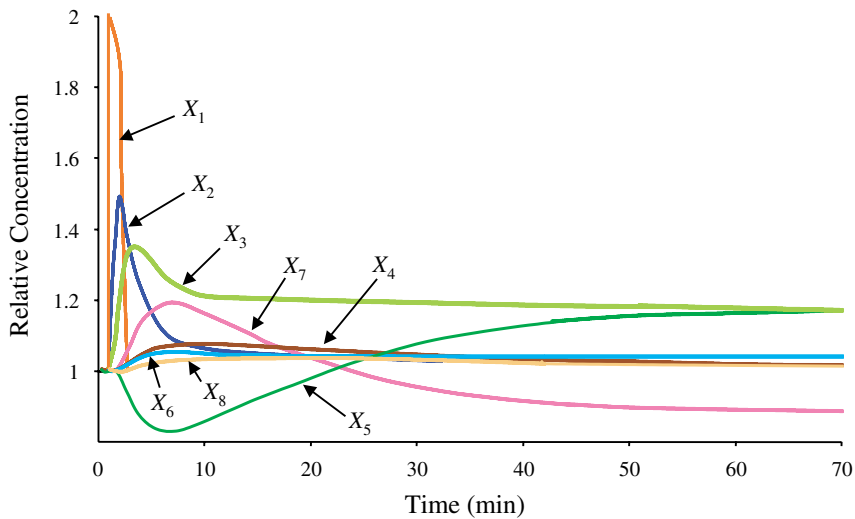
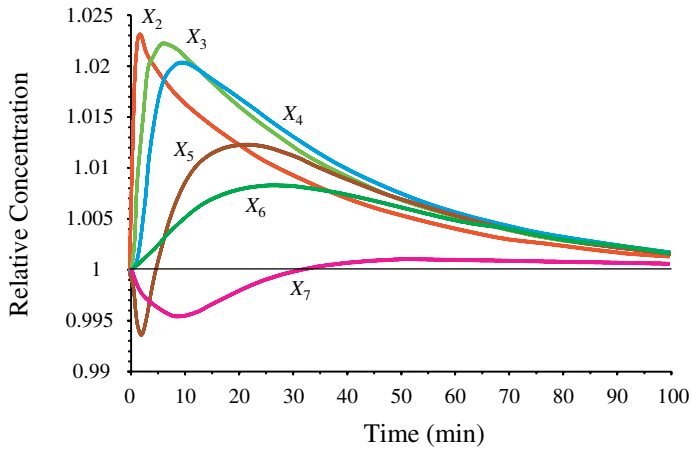


**Figure 2.6.** Schematic illustration of a Monte-Carlo simulation. Three independent (input) variables  $X_{n+1}$ ,  $X_{n+2}$ , and  $X_{n+3}$ , are distributed as shown on the left. Their distributions lead to output, such as  $X_1$ ,  $X_2$ ,  $X_3$ , and  $X_4$ , that is also distributed. The output distributions may have a variety of shapes that depend on the model and are often difficult to predict without an actual execution of the simulation.



**Figure 3.10.** Dynamic system response to a twofold increase in glucose 6-phosphate ( $X_1$ ). At time 1, the glucose 6-phosphate pool ( $X_1$ ) was increased to twice the steady state. The eight metabolites represented are glucose 6-phosphate ( $X_1$ ), fructose 6-phosphate ( $X_2$ ), phosphoenol pyruvate ( $X_3$ ), pyruvate ( $X_4$ ), oxalacetate ( $X_5$ ), malate ( $X_6$ ), NADH ( $X_7$ ), and ATP ( $X_8$ ). Each concentration is normalized with respect to its nominal steady-state value. The long time scale of the response is cause for concern.



**Figure 3.18.** Dynamic system response to a twofold increase in cytosolic glucose ( $X_1$ ). At time zero, the cytosolic glucose pool ( $X_1$ ) was increased to twice the steady state. The six metabolites represented are glucose 6-phosphate ( $X_2$ ), fructose 6-phosphate ( $X_3$ ), fructose-2,6-bisphosphate ( $X_4$ ), phosphoenol pyruvate ( $X_5$ ), cytosolic pyruvate ( $X_6$ ), and cytosolic oxalacetate ( $X_7$ ). The remaining metabolites exhibit negligible deviations from the basal steady-state values (below 0.5%). Each concentration is normalized with respect to its nominal steady-state value. The response in the revised model is much improved over the initial model (compare y axis with Figure 3.10).

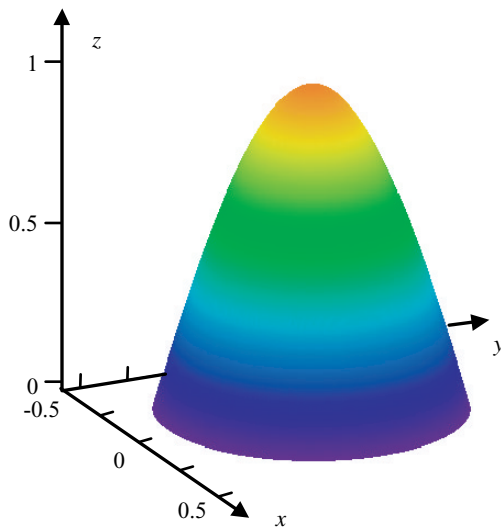


**Figure 4.6.** The graph of the two-variable function  $z = 3 - 2 \cdot \sqrt{1 + 6.25 \cdot (x^2 + y^2)}$  is a smooth surface.

**Figure 4.7.** The intersection of the graph in Figure 4.6 and the plane  $x = 0.22$  shows the projection of  $z = f(0.22, y)$ , which now is a univariate function of  $y$ .

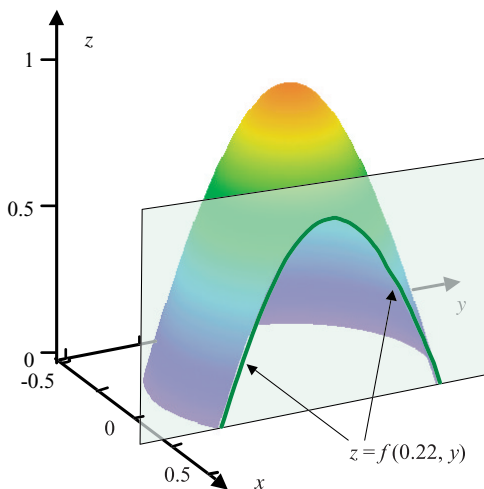


**Figure 4.8.** The center of the saddle is characterized by a zero gradient, yet this center is not a maximum or minimum. It is minimal in  $x$ -direction and maximal in  $y$ -direction.

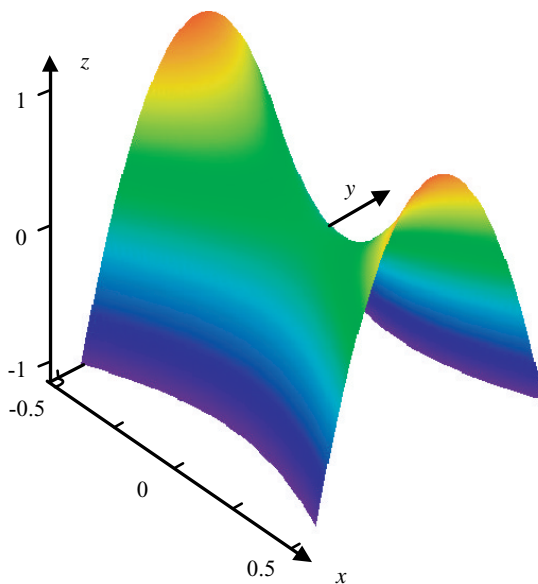


**Figure 4.9.** Paraboloid described in Eq. (4.47). The wire mesh shows the  $x$ - $y$  plane. The intersection between the paraboloid and the solid plane is the circle of constrained minima.

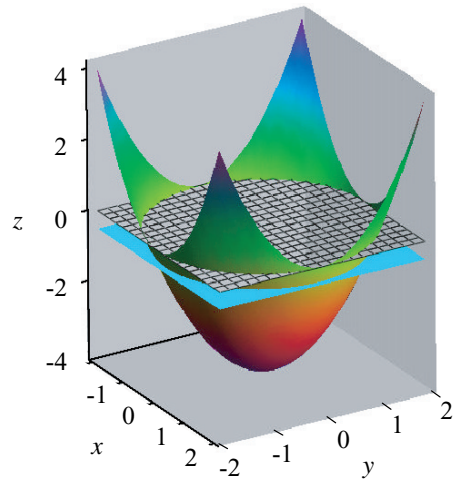


**Figure 4.12.** Three paths,  $C_1$ ,  $C_2$ , and  $C_3$ , run along a three-dimensional surface, defined by the function  $f$ . They intersect at point  $P$ , where their tangents,  $T_1$ ,  $T_2$ , and  $T_3$ , along with the tangents of all other paths intersecting at  $P$ , form the tangent plane at  $P$ . The gradient is perpendicular to the tangent plane at  $P$ .

